fibers

Article

Compression of Few-Microjoule Femtosecond Pulses in a Hollow-Core Revolver Fiber

Leonid Losev [1], Vladimir Pazyuk [1], Alexey Gladyshev [2,*], Yury Yatsenko [2], Alexey Kosolapov [2] and Igor Bufetov [2]

[1] P.N. Lebedev Physical Institute, Russian Academy of Sciences, Leninsky Prosp. 53, Moscow 119991, Russia
[2] Dianov Fiber Optics Research Center, Prokhorov General Physics Institute of the Russian Academy of Sciences, 38 Vavilov St., Moscow 119333, Russia
* Correspondence: alexglad@fo.gpi.ru

Abstract: Gas-filled hollow-core fibers are a convenient tool for laser pulse compression down to a few-cycle duration. The development of compact, efficient and high quality compression schemes for laser pulses of relatively low μJ-level energies is of particular interest. In this work, temporal pulse compression based on nonlinear spectral broadening in a xenon-filled revolver fiber followed by a chirped mirror system is investigated. A 250 fs pulse at a central wavelength of 1.03 μm is compressed to 13.3 fs when the xenon pressure was tuned to provide zero group velocity dispersion near 1.03 μm. The energies of input and compressed pulses are 3.8 and 2.7 μJ, respectively. The compression quality factor of 1.8 is achieved.

Keywords: hollow-core fiber; few-cycle pulse; self-phase modulation; nonlinear spectral broadening; chirped mirror; temporal pulse compression

check for updates

Citation: Losev, L.; Pazyuk, V.; Gladyshev, A.; Yatsenko, Y.; Kosolapov, A.; Bufetov, I. Compression of Few-Microjoule Femtosecond Pulses in a Hollow-Core Revolver Fiber. *Fibers* **2023**, *11*, 22. https://doi.org/10.3390/fib11020022

Academic Editor: Vladimir Volkov

Received: 29 December 2022
Revised: 1 February 2023
Accepted: 14 February 2023
Published: 20 February 2023

1. Introduction

In recent years, microstructured hollow-core fibers (HCF) have been widely used in nonlinear optics experiments with low-power laser pulses. In spite of low power, the pulse intensity could reach high values due to the small diameter of the hollow core. Moreover, low propagation losses in modern hollow-core fibers allow a long interaction length, which facilitates nonlinear processes. The optical power required to reach the threshold of nonlinear processes can be decreased most strongly for those phenomena in which the key parameter is the product of the optical intensity and the interaction length. Typical cases of such phenomena are stimulated Raman scattering (SRS) and spectral broadening induced by nonlinear self-phase modulation (SPM). For example, the use of hollow-core microstructured fibers enabled efficient Raman conversion in compressed gases even for optical pulses with energy as low as several μJ [1].

The SPM-induced nonlinear spectral broadening of the laser pulses is widely used for temporal pulse compression. To achieve compression of femtosecond pulses to a few-cycle duration, the hollow-core fiber must provide low optical losses in a spectral range that is wide enough to support propagation of all frequencies composing a few-cycle pulse. Such a requirement is satisfied in broadband-guiding hollow-core fibers, the transmission spectrum of which are determined not by a photonic band gap of the cladding, but by antiresonant reflection of the propagating wave from thin glass struts that form the core-cladding interface [2,3].

The antiresonant HCFs have a transmission spectrum that consists of a set of low-loss transmission bands, which can be as wide as ~1000 nm. The spectral bandwidth and position of the transmission bands are defined by the thickness of silica glass struts on the core-cladding interface. However, the antiresonant guiding mechanism cannot explain all the optical properties of such fibers. In particular, the level of optical losses that was experimentally obtained in broadband-guiding hollow-core fibers appeared to be much less compared to predictions that followed from the antiresonant guiding model. As an attempt to resolve this discrepancy, an alternative guiding mechanism was proposed based on the idea of inhibited coupling between a core mode and cladding modes that have the same effective index of refraction [4]. Although the inhibited coupling mechanism was implemented to explain the waveguiding properties of Kagome-lattice hollow-core fibers, this mechanism moreover does not provide a complete picture. This fact became clear when two research groups discovered independently that the *shape* of the core-cladding interface has a strong influence on the level of optical losses in broadband-guiding hollow-core fibers [5,6]. The introduction of a negative curvature of the core-cladding boundary into the antiresonant fibers helped to significantly improve the localization of the light in the hollow core [5–9]. As a result, the optical losses in the antiresonant HCFs were reduced significantly, thus boosting the practical applications of such fibers [9–11]. The effect of the negative curvature of the core-cladding boundary on the optical loss reduction was also demonstrated using other cross-sectional designs of the hollow-core fibers (such as "ice cream" [12] and "nested" [13,14] HCFs).

At the same time, each transmission band of the broadband-guiding hollow-core fibers included a zero-dispersion wavelength (λ_{ZDW}), at which the group velocity dispersion β_2 vanishes, and most of the transmission band falls into the region of anomalous dispersion [2,3,15]. Importantly, the anomalous dispersion of the fiber is comparable in magnitude with the positive dispersion of various gases. This fact makes it possible to control the dispersion of antiresonant HCFs by changing the composition and pressure of the gas that fills the hollow core [2].

The most practical type of negative-curvature antiresonant HCFs are revolver fibers [5,7,8]. Due to their simple design and unique optical properties, the revolver fibers have attracted much attention and are now studied for various applications, including extreme compression of femtosecond pulses to single-cycle duration [16,17].

Two schemes of femtosecond pulse compression in gas-filled HCFs can be distinguished: (1) self-compression of the pulses propagating in the anomalous dispersion region of the fiber and (2) pulse compression on external optical elements with negative dispersion when the pulse propagates in the normal dispersion region of the fiber.

Despite its simplicity, the first scheme usually suffers from the low compression quality, which is described by the quality factor Q_C, defined as the ratio of the energy in the compressed part of the pulse to the energy of the uncompressed pedestal. For laser pulses with a duration greater than 100 fs, the quality factor can be expressed as $Q_C \approx 1/F_C$, where the compression factor F_C is the ratio of the initial pulse duration to the compressed pulse duration [18]. Thus, the higher is the compression factor F_C and the lower is the compression quality Q_C, which means that a significant fraction of the pulse energy at the exit of the hollow-core fiber will be contained in a low-intensity pedestal that has a duration close to the duration of the initial laser pulse. This fact limits the application of such a compressor significantly. Therefore, compression schemes based on external optical elements with negative dispersion are more attractive when the quality of compressed pulses is of high importance.

In the second scheme of pulse compression, in which the pulse propagates in the normal dispersion region of the fiber, the SPM-induced spectral broadening for pulses with a fixed energy can be increased by increasing the gas pressure and, consequently, the nonlinear refractive index n_2. However, in this case, effects associated with the dispersion of the active medium could produce a detrimental impact on the compression process. Effects such as a steepening of the trailing edge of the pulse [19], and dispersive spreading of the pulse, in time lead to a nonlinear pulse chirp at the output of the HCF and require an increase in the negative dispersion of the optical elements at the compressor output. As a result, the compression quality may decrease.

In this work, we study the influence of the xenon-filled HCF dispersion on the spectral broadening of femtosecond laser pulses in order to develop a simple compressor scheme that allows high-quality compression of a few-μJ-level pulses to a few-cycle duration. By using a single-step spectral broadening in xenon-filled revolver fibers with post-compression on chirped mirrors, 250 fs pulses of an ytterbium laser with a pulse energy of 3.8 µJ are compressed to a duration as low as ~13 fs with the energy efficiency as high as 71%. The combination of pulse duration and compression quality achieved in this work is not possible in the gas-filled capillaries [20] and requires more complex two-step compression schemes in the case of gas-filled hollow-core fibers [17].

2. Materials and Methods

The scheme of the experimental setup is shown in Figure 1. A femtosecond ytterbium laser TETA (Avesta) was used as a source of ~250 fs pulses with a repetition rate of up to 500 kHz at the wavelength of 1.03 µm. The built-in pulse compressor that was installed at the laser output allowed for changing the pulse duration if needed. The output beam had a Gaussian intensity distribution with a diameter of 2.5 mm. The laser beam was focused into the hollow core of a revolver fiber (Figure 1, red horizontal line) by the lens L1 with a focal length of 4 cm. The fiber was completely placed in a 52-cm-long chamber, which was filled with xenon. Since we are interested in achieving the nonlinear pulse compression at the lowest possible pump pulse energy, we facilitated the nonlinear spectral broadening by using the longest length of the revolver fiber available in our setup, i.e., the fiber length was fixed at 50 cm. The xenon pressure was varied in the experiments to find the optimal conditions for nonlinear spectral broadening. At the chamber exit, the beam was collimated by the lens L2 and launched into a pulse compressor consisting of two chirped mirrors, M1 and M2, with a negative group delay dispersion. At the output of the pulse compressor, the spectrum of the pulse was recorded by an ASP75 spectrometer (Avesta), and the pulse duration was measured with an ASF5 autocorrelator (Avesta).

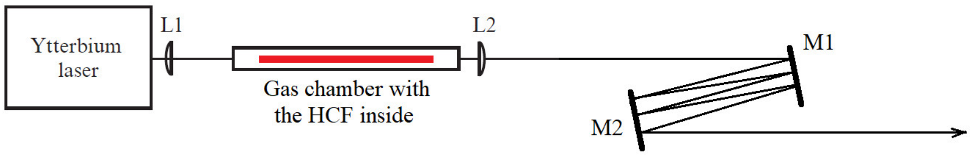

Figure 1. The scheme of the experimental setup. L1, L2—lenses. M1, M2—chirped mirrors. Red line is the HCF placed inside a gas chamber.

A revolver hollow-core fiber fabricated at FORC RAS was used for the experiments (Figure 2a, left inset). The fiber has a hollow-core diameter of 36 µm and a fundamental mode field diameter of 26 μm^2. The fiber cladding is formed by 9 capillaries that have the diameter of 14 µm and a wall thickness of 0.75 µm. Variations of the hollow-core fiber geometrical parameters were no more than 2%. The optical loss spectrum in the range of 0.8–1.3 µm was calculated by the finite element method for a fundamental and a few higher-order modes of the fiber (Figure 2a). The pump wavelength (1.03 µm) used in the experiments is located in the center of the fiber transmission band, where an optical loss of 12.6 dB/km was calculated for the fundamental mode. Determined at the loss level of 0.1 dB/m, the spectral width of the transmission band was as wide as 350 nm for the fundamental mode of the HCF. The spectrum of optical losses is not smooth at the long wavelength edge of the fiber transmission band. This effect is due to resonant coupling between the core and cladding modes. Since such mode coupling is different for different propagating modes, the smoothness of the optical loss spectra depends on the particular mode under consideration.

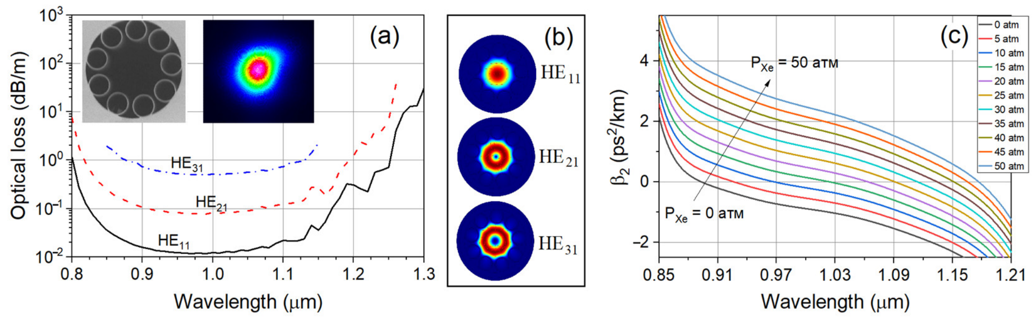

Figure 2. (**a**) Optical loss spectrum calculated for the fundamental (HE_{11}) and two higher-order modes of the fiber (HE_{21} and HE_{31}). The SEM-image of the revolver fiber cross-section is shown on the left inset. Near-field intensity distribution measured at the fiber output is shown on the right inset. (**b**) The calculated intensity distributions for the lowest order modes (HE_{11}, HE_{21}, HE_{31}) of the fiber. (**c**) Group velocity dispersion β_2 of the fundamental mode as a function of wavelength at various xenon pressures.

The group velocity dispersion β_2 as a function of wavelength was calculated for different pressures of Xe, taking into account both xenon dispersion [21] and waveguide dispersion of the HCF fundamental mode (Figure 2c). The zero dispersion wavelength shifts from 0.89 to 1.18 μm as the xenon pressure increases from 0 to 50 atm (Figure 3a). The quadratic dispersion at pump wavelength (1.03 μm) increases monotonically with pressure, reaching the zero value at a xenon pressure of 15 atm and a maximum value of +2.23 ps^2/km at a pressure of 50 atm (Figure 3b).

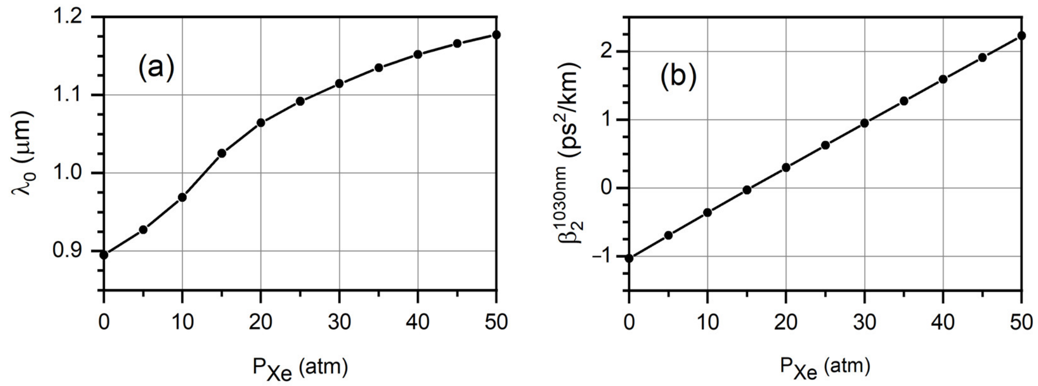

Figure 3. (**a**) Zero dispersion wavelength λ_0 as a function of xenon pressure for the fundamental mode of the fiber. (**b**) Group velocity dispersion β_2 for the fundamental mode at a pump wavelength of 1.03 μm as a function of the xenon pressure.

3. Results and Discussion

The pulse spectra at the output of the revolver fiber were measured at various input pulse energies and xenon pressures. Qualitatively different spectra were observed at xenon pressures of 15 and 40 atm (Figure 4), which correspond to the zero dispersion (β_2 = 0) and all-normal dispersion case, respectively. By the zero dispersion case, we mean the case when the xenon pressure is chosen so that the value of dispersion β_2 equals zero at the laser wavelength (1.03 μm). In turn, the all-normal dispersion case implies that gas pressure is high enough to provide a positive value of β_2 in the whole spectral range involved in the experiment.

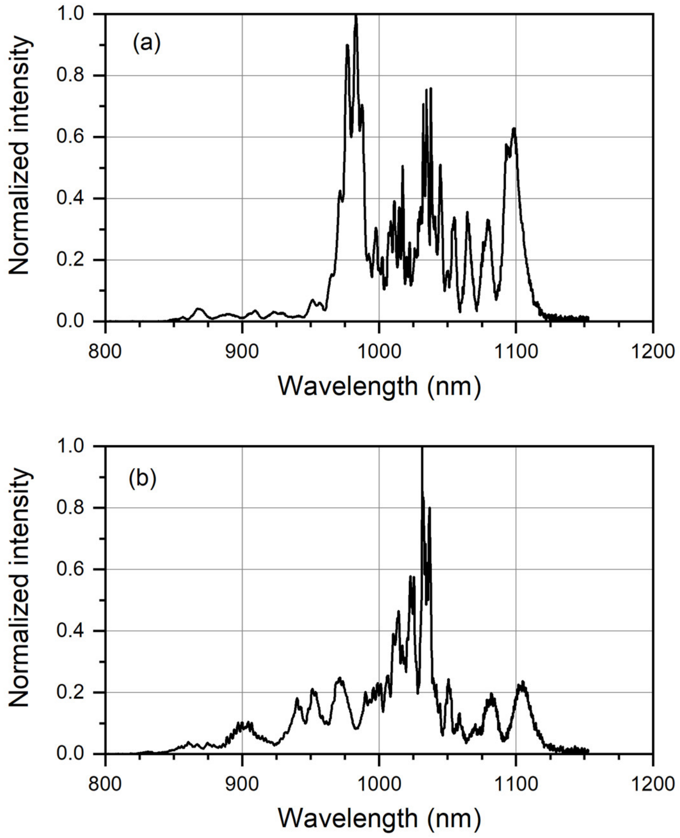

Figure 4. Typical spectra measured at the revolver fiber output for (**a**) xenon pressure of 15 atm and input pulse energy of 3.8 μJ, and (**b**) xenon pressure of 40 atm and input pulse energy of 1.5 μJ.

For the case of zero dispersion at 1.03 μm, the output spectrum has a symmetrical shape with intensity increasing at the edges of the spectrum (Figure 4a), which is the classical spectral shape induced by pure self-phase modulation without changes of the pulse shape and duration. A different spectral shape is observed at a xenon pressure of 40 atm (Figure 4b). In this case, the spectrum becomes asymmetric with respect to the central wavelength of the initial laser pulse (1.03 μm) and shifts to the short wavelength region. Such a transformation of the output spectrum is typical when self-phase modulation is accompanied by self-steepening of the trailing edge of the pulse, resulting in an intense short-wavelength component [19]. Self-steepening of optical pulses is a consequence of the intensity dependent group velocity dispersion, which increases with xenon pressure. Although pulse self-steepening can produce wider spectra, it does not help in achieving extremely short pulses at the post-compression stage. The frequency chirp of the pulse during the steepening of the trailing edge becomes significantly nonlinear and, as a consequence, the compression quality drops sharply.

Although optical pulses at the hollow-core fiber output have wide spectra (Figure 4), the pulse duration is far from a transform-limited value, and the use of the mirror-based post-compressor is necessary in order to shape the pulses in time. Based on the measured output spectra, we have calculated the transform-limited pulse duration that can be potentially obtained after the pulses will pass the external compressor based on chirped mirrors (see Figure 1). Figure 5 shows the calculated transform-limited pulse duration as a function of the input pulse energy for xenon pressures of 15 atm (Figure 5a) and 40 atm (Figure 5b). The calculated values present the shortest pulse durations that can be achieved at the output of an external pulse compressor based on chirped mirrors. The figures also show the energy transmission through the fiber, which is equal to the ratio of the pulse energy at the fiber output to the energy of the input pulse. Both propagation losses and efficiency of energy coupling into the hollow core contribute to the transmission of the fiber.

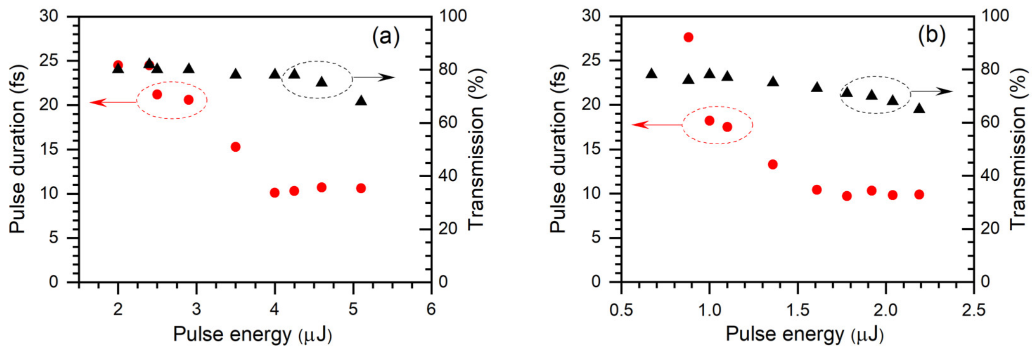

Figure 5. The transform-limited pulse duration (circles) calculated from the experimentally observed spectral width of the pulses as a function of input pulse energy. The fiber transmission (triangles) as a function of the input pulse energy. The size of experimental points corresponds to the error bar of the measurements. The pressure of xenon was 15 atm (**a**) and 40 atm (**b**).

The duration of transform-limited pulses decreases with the input pulse energy due to SPM-induced spectral broadening of propagating pulses (Figure 5). Starting at a certain pulse energy, the transform-limited pulse duration reaches a minimal value of about 10 fs and does not change with further energy growth of input pulses. Note, the minimal pulse duration has the same value for both zero dispersion (Figure 5a) and all-normal dispersion (Figure 5b) cases. Such a dependence may indicate that the spectral width of output pulses is limited by some mechanism, which could be the bandwidth of the HCF transmission band (Figure 2a).

The assumption above is confirmed by the following facts. First, the energy transmission of the fiber starts dropping down when the pulse duration limit is reached (Figure 5). Of note, the transmission decrease cannot be caused by self-focusing of the propagating pulse, as the critical power required for self-focusing in the xenon at a pressure of 40 atm is equal to ~50 MW [22], while no more than 10 MW of peak power was used in the experiments at this pressure.

The second observation is that the pulse energy E_p (and, consequently, the pulse intensity I_p), at which the pulse duration reaches the minimal value, was observed to be inversely proportional to xenon pressure E_p~I_P~$1/P_{Xe}$. For example, pulse energies of 4 and 1.5 μJ were required to reach the 10 fs duration limit at xenon pressures of 15 and 40 atm, respectively. At the same time, the nonlinear refractive index n_2 is proportional to xenon pressure n_2~P_{Xe}. Thus, the strongest spectral broadening $\Delta\omega$ induced by SPM is independent on gas pressure ($\Delta\omega \sim I_p \times n_2 = \text{const}$), which means that the shortest possible duration of transform-limited pulses should be the same for any xenon pressure.

Importantly, the low loss transmission band of the HCF calculated for the fundamental mode is as high as 350 nm (Figure 2a), while the pulse duration limit of 10 fs for sech^2-shaped pulses corresponds to a pulse bandwidth of only about 100 nm. What prevents the nonlinear spectral broadening to cover the whole transmission band of the fiber is not absolutely clear. A possible explanation for this discrepancy could be an excitation of higher-order modes when coupling the laser beam into the hollow-core fiber. Indeed, if a non-negligible fraction of input pulse energy is launched into the higher-order modes, the effective transmission bandwidth of the HCF will be reduced since higher-order modes have narrower transmission bands compared to the fundamental mode, as can be seen in Figure 2a. To check this assumption, the near-field beam profile was measured (Figure 2a, right inset). Although a Gaussian-like beam profile was observed, the excitation of the higher-order modes cannot be excluded, since the most easily excited higher-order modes such as HE_{21} and HE_{31} have a donut-shaped intensity distribution (Figure 2b), which makes it difficult to distinguish the higher-order modes in the presence of the fundamental mode. Therefore, in our experimental conditions, the minimum possible duration of a compressed pulse is about 10 fs, and we believe this value is determined by the transmission bandwidth of the fiber, taking into account excitation of higher-order modes. More detailed studies accompanied by numerical simulations are required to clarify this point.

Experiments on the temporal compression of spectrally broadened pulses were carried out using a multi-pass system of two chirped mirrors at the HCF output. The chirped mirrors (Layertec) were 40×10 mm^2 in size and had a group dispersion delay value of about -100 fs^2 in the spectral range of 920–1150 nm. The maximum of 20 reflections from the surface of the mirrors was possible in our experimental conditions at a distance between the mirrors of 12 cm. The power transmission through the chirped mirror system exceeded 90%.

By optimizing the number of reflections when operating in the zero dispersion region at a xenon pressure of 15 atm, the output pulse was compressed to a duration of 13.3 fs (Figure 6a). The number of reflections in this case was 10, and the introduced value of the group delay dispersion was about -1000 fs^2. Calculations show that this dispersion value is sufficient for a positively chirped 220-fs-long pulse that has a spectrum corresponding to a 10-fs-long sech^2-shaped pulse, and can be compressed to its transform-limited value of 10 fs. These estimates are in good agreement with the experimental data. Uncompensated nonlinear chirp of the output pulses could be the reason for the pedestal that was observed in autocorrelation traces (Figure 6).

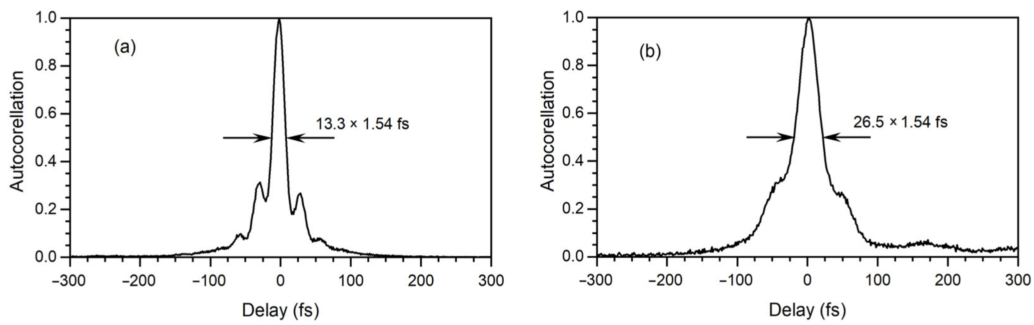

Figure 6. Autocorrelation functions of compressed pulses. Xenon pressure, input pulse energy, number of reflections from chirped mirrors were (**a**) 15 atm, 3.8 µJ, 10 and (**b**) 40 atm, 1.5 µJ, 20, respectively.

The energy of the laser pulse at the entrance to the HCF varied within 3.8–4.0 µJ. Taking into account the transmission of the chirped mirrors system, the energy efficiency of the compressor as a whole was 70%. The compression quality factor in this case was $Q_C \approx 1.8$, which corresponds to the compression quality for a phase-modulated Gaussian pulse [23]. A further increase in the laser pulse energy led to a decrease in the compression quality, while maintaining the duration of the pulse peak. This effect can be related to the fact that the width of the pulse spectrum begins to exceed the spectral band of the chirped mirrors used. For example, at a laser pulse energy of 5 µJ, the compression quality dropped to 1.

Similar results were obtained when the xenon pressure was varied in the range of 15–20 atm, which is close to a zero dispersion regime of pulse propagation. However, for the xenon pressures higher than 20 atm, the dispersive spreading of the pulse becomes significant, and a larger number of reflections from chirped mirrors is required to compress the pulse in time, since a larger value of the group delay dispersion needs to be compensated. In particular, at the maximum xenon pressure realized in the experiment (40 atm), the number of reflections from chirped mirrors has to be increased up to the maximum possible value, which is 20 in our experimental conditions. In this case, the shortest pulse duration was measured to be 26 fs (Figure 6b), which is limited by a net value of the negative group delay dispersion that can be achieved in our chirped mirror system. The energy of the laser pulse was 1.5 µJ. As estimates [24] show, in this case, the duration of the pulse with the spectrum shown in Figure 4b increases to ~500 fs at the fiber output, which makes it necessary to increase the introduced value of the negative group delay dispersion above the maximum value available in our setup.

One should note that chirped mirrors as negative dispersion elements for temporal pulse compression enable high energy efficiency of the compressor and small overall dimensions of the device. Importantly, the value of a negative group delay that is introduced by a reflection from a chirped mirror decreases with increasing the spectral bandwidth of the mirror. Then, to obtain few-cycle optical pulses with a high compression quality, it is desirable to use as short pulses as possible at the input to the chirped mirror system. In a hollow-core fiber compressor, this can be done by operating in the zero group velocity dispersion region by selecting the gas pressure. In this case, the pulse energy variation should be accompanied by a change in the length of the hollow-core fiber.

4. Conclusions

Temporal pulse compression based on single-step nonlinear spectral broadening in a xenon-filled revolver fiber followed by a chirped mirror system is investigated. The maximum compression of femtosecond pulses is achieved at a xenon pressure of 15 atm that tunes a zero dispersion wavelength to match the central wavelength of the input pulse ($\lambda_{ZDW} \approx 1.03$ μm). A 250 fs ytterbium laser pulse is compressed to 13.3 fs. The energies of input and compressed pulses were 3.8 and 2.7 μJ, respectively, demonstrating an energy efficiency of 71%. The compression quality factor, i.e., the ratio of the energy in the compressed part of the pulse to the energy of the uncompressed pedestal, was about 1.8.

The results obtained show a valuable improvement compared with previous results in xenon-filled capillaries [20], where achieving the shortest duration of a compressed pulse (17 fs) was inevitably accompanied by energy efficiency reduction (down to 40%). By providing low optical loss and more freedom in dispersion control, the gas-filled revolver fibers allow shorter pulses to be achieved without compromising the energy efficiency of pulse compression. A few works based on gas-filled hollow-core fibers had demonstrated pulse compression to shorter duration compared with the current work; however, those results were achieved in a two-step compression scheme, which adds significantly to the system complexity [17].

Author Contributions: Conceptualization, L.L. and V.P.; methodology, L.L. and V.P.; software, Y.Y.; validation, L.L., V.P., Y.Y. and A.G.; formal analysis, L.L. and Y.Y.; investigation, L.L. and V.P.; resources, A.K.; data curation, L.L., Y.Y. and A.G.; writing—original draft preparation, L.L.; writing—review and editing, all coauthors; visualization, L.L. and A.G.; supervision, L.L., A.G. and I.B.; project administration, I.B.; funding acquisition, I.B. All authors have read and agreed to the published version of the manuscript.

Funding: This research was supported by the Russian Science Foundation (grant No. 19-12-00361). https://rscf.ru/en/project/19-12-00361/ (accessed on 27 December 2022).

Data Availability Statement: The data that support the findings of this study are available from the corresponding author, A.G., upon reasonable request.

Conflicts of Interest: The authors declare no conflict of interest.

References

1. Chafer, M.; Osório, J.H.; Dhaybi, A.; Ravetta, F.; Amrani, F.; Delahaye, F.; Debord, B.; Cailteau-Fischbach, C.; Ancellet, G.; Gérôme, F.; et al. Near- and middle-ultraviolet reconfigurable Raman source using a record-low UV/visible transmission loss inhibited-coupling hollow-core fiber. *Opt. Laser Technol.* **2022**, *147*, 107678. [CrossRef]
2. Russell, P.S.J.; Hölzer, P.; Chang, W.; Abdolvand, A.; Travers, J.C. Hollow-core photonic crystal fibres for gas-based nonlinear optics. *Nat. Photonics* **2014**, *8*, 278–286. [CrossRef]
3. Yu, F.; Knight, J.C. Negative Curvature Hollow-Core Optical Fiber. *IEEE J. Sel. Top. Quantum Electron.* **2016**, *22*, 146–155. [CrossRef]
4. Couny, F.; Benabid, F.; Roberts, P.J.; Burnett, M.T.; Maier, S.A. Identification of Bloch-modes in hollow-core photonic crystal fiber cladding. *Opt. Express* **2007**, *15*, 325–338. [CrossRef]
5. Pryamikov, A.D.; Biriukov, A.S.; Kosolapov, A.F.; Plotnichenko, V.G.; Semjonov, S.L.; Dianov, E.M. Demonstration of a waveguide regime for a silica hollow-core microstructured optical fiber with a negative curvature of the core boundary in the spectral region >3.5 μm. *Opt. Express* **2011**, *19*, 1441–1448. [CrossRef] [PubMed]
6. Wang, Y.Y.; Wheeler, N.V.; Couny, F.; Roberts, P.J.; Benabid, F. Low loss broadband transmission in hypocycloid-core Kagome hollow-core photonic crystal fiber. *Opt. Lett.* **2011**, *36*, 669–671. [CrossRef] [PubMed]

7. Kolyadin, A.N.; Kosolapov, A.F.; Pryamikov, A.D.; Biriukov, A.S.; Plotnichenko, V.G.; Dianov, E.M. Light transmission in negative curvature hollow core fiber in extremely high material loss region. *Opt. Express* **2013**, *21*, 9514–9519. [CrossRef] [PubMed]
8. Bufetov, I.A.; Kosolapov, A.F.; Pryamikov, A.D.; Gladyshev, A.V.; Kolyadin, A.N.; Krylov, A.A.; Yatsenko, Y.P.; Biriukov, A.S. Revolver Hollow Core Optical Fibers. *Fibers* **2018**, *6*, 39. [CrossRef]
9. Debord, B.; Amrani, F.; Vincetti, L.; Gérôme, F.; Benabid, F. Hollow-Core Fiber Technology: The Rising of "Gas Photonics". *Fibers* **2019**, *7*, 16. [CrossRef]
10. Markos, C.; Travers, J.C.; Abdolvand, A.; Eggleton, B.J.; Bang, O. Hybrid photonic-crystal fiber. *Rev. Mod. Phys.* **2017**, *89*, 045003. [CrossRef]
11. Wei, C.; Weiblen, R.J.; Menyuk, C.R.; Hu, J. Negative curvature fibers. *Adv. Opt. Photon.* **2017**, *9*, 504–561. [CrossRef]
12. Yu, F.; Wadsworth, W.J.; Knight, J.C. Low loss silica hollow-core fibers for 3–4 μm spectral region. *Opt. Express* **2012**, *20*, 11153–11158. [CrossRef] [PubMed]
13. Belardi, W.; Knight, J.C. Hollow antiresonant fibers with reduced attenuation. *Opt. Lett.* **2014**, *39*, 1853–1856. [CrossRef] [PubMed]
14. Poletti, F. Nested antiresonant nodeless hollow core fiber. *Opt. Express* **2014**, *22*, 23807–23828. [CrossRef] [PubMed]
15. Zeisberger, M.; Hartung, A.; Schmidt, M. Understanding Dispersion of Revolver-Type Anti-Resonant Hollow Core Fibers. *Fibers* **2018**, *6*, 68. [CrossRef]
16. Balciunas, T.; Fourcade-Dutin, C.; Fan, G.; Witting, T.; Voronin, A.A.; Zheltikov, A.M.; Gerome, F.; Paulus, G.G.; Baltuska, A.; Benabid, F. A strong-field driver in the single-cycle regime based on self-compression in a kagome fibre. *Nat. Commun.* **2015**, *6*, 6117. [CrossRef]
17. Köttig, F.; Schade, D.; Koehler, J.R.; Russell, P.S.J.; Tani, F. Efficient single-cycle pulse compression of an ytterbium fiber laser at 10 MHz repetition rate. *Opt. Express* **2020**, *28*, 9099–9110. [CrossRef]
18. Schade, D.; Köttig, F.; Koehler, J.R.; Frosz, M.H.; Russell, P.S.J.; Tani, F. Scaling rules for high quality soliton self-compression in hollow-core fibers. *Opt. Express* **2021**, *29*, 19147–19158. [CrossRef]
19. Anderson, D.; Lisak, M. Nonlinear asymmetric pulse distortion in long optical fibers. *Opt. Lett.* **1982**, *7*, 394–396. [CrossRef]
20. Didenko, N.V.; Konyashchenko, A.V.; Kostryukov, P.V.; Losev, L.L.; Pazyuk, V.S.; Tenyakov, S.Y.; Bryukhanov, V.V. Temporal compression of pulses from a 100-kHz-repetiton-rate femtosecond ytterbium laser. *Quantum Electron.* **2016**, *46*, 675–678. [CrossRef]
21. Borzsonyi, A.; Heiner, Z.; Kalashnikov, M.P.; Kovacs, A.P.; Osvay, K. Dispersion measurement of inert gases and gas mixtures at 800 nm. *Appl. Opt.* **2008**, *47*, 4856–4863. [CrossRef] [PubMed]
22. Lo, S.-Z.A.; Wang, L.; Lon, Z.-H. Pulse propagation in hollow-core fiber at high-pressure regime: Application to compression of tens of μJ pulses and determination of nonlinear refractive index of xenon at 1.03 μm. *Appl. Opt.* **2018**, *57*, 4659–4664. [CrossRef] [PubMed]
23. Konyashchenko, A.V.; Kostryukov, P.V.; Losev, L.L.; Tenyakov, S.Y. Capillary compressor of femtosecond pulses with nonlinear rotation of polarization ellipse. *Quantum Electron.* **2012**, *42*, 231–234. [CrossRef]
24. Didenko, N.V.; Konyashchenko, A.V.; Losev, L.L.; Pazyuk, V.S. Compression of femtosecond laser pulses based on supercritical xenon. *Quantum Electron.* **2018**, *48*, 621–624. [CrossRef]